Supporting Information

Deep-UV Emission from Highly-Ordered AlGaN/AlN Core-Shell Nanorods

Pierre-Marie Coulon[*,1], *Gunnar Kusch*[2], *Robert W. Martin*[2] *and Philip A. Shields*[1]

[1]Centre of Nanoscience & Nanotechnology, University of Bath, Bath, BA2 7AY, UK

Department of Electronic and Electrical Engineering, University of Bath, Bath, BA2 7AY, UK

[3]Department of Physics, SUPA, University of Strathclyde, Glasgow, G4 0NG, UK.

*E-mail: P.Coulon@bath.ac.uk

S1: Displacement Talbot Lithography patterning

Displacement Talbot lithography (DTL) is a recently developed technique for patterning large areas with sub-micron periodic features.[1] It is an extension of Talbot lithography, which uses the three-dimensional interference pattern created when monochromatic light diffracts through a periodic mask. The introduction of a displacement during exposure along the axis perpendicular to the mask, integrates the optical field which leads to a theoretical infinite depth of field.

Figure S1 shows the hexagonal array of hole patterned in resist after DTL exposure and development, which consisted of ~260 nm diameter openings. The white halo surrounding the openings indicates the successful formation of an undercut profile in the underlying bottom antireflective layer.

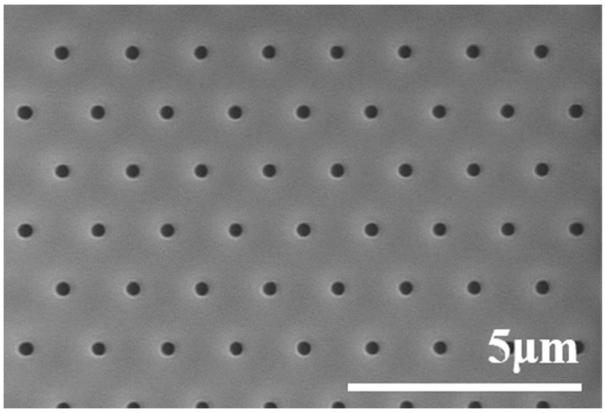

Figure S1. Secondary-electron SEM images of the hole pattern in resist after DTL exposure and development.

S2: Lift-off

Figure S2 shows the hexagonal array of Au/Ni metal dot mask obtained after lift-off, which consisted of ~250 nm diameter dots.

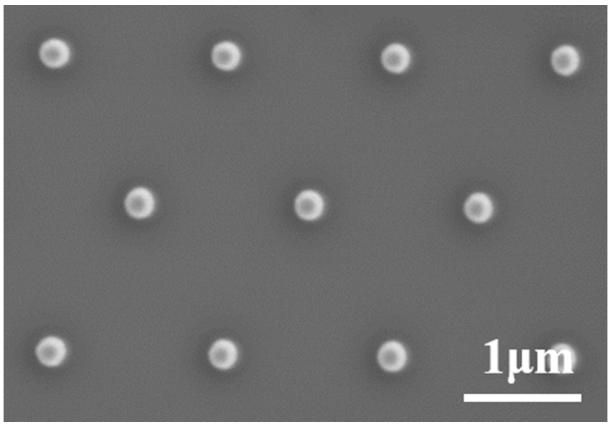

Figure S2. Secondary-electron SEM images of the Au/Ni metal dot mask after lift-off.

S3: Two step dry-etching

Figure S3.a shows AlN nanorod arrays after ICP dry etching and cleaning, which present a small undercut. Figure S3.b shows AlN nanorod arrays after the two step ICP dry etching and AZ400K potassium hydroxide (KOH) based wet etching. The additional wet etching step allows to achieve a smooth and straight sidewall profile. It also induces a decrease of the nanorod diameter. Note that the circular trenches induced by ICP dry etching at the bottom part of the nanorod seems to follow a preferential faceted etching after KOH wet etching. While the wet etching seems to be driven along the 10-10 direction, no clear formation of plane can unambiguously made within the trenches.

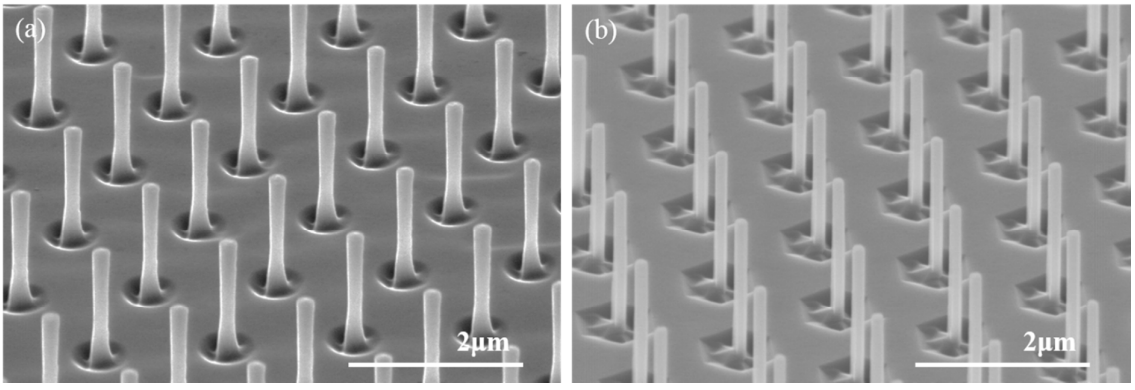

Figure S3. Cross-section SEM images of (a) AlN nanorod arrays after ICP dry etching and (b) AlN nanorod after subsequent AZ400K wet etching.

S4: TEM observation

Figure S4 displays scratched AlN nanorod after the two-step dry-wet etching. One threading dislocation (TD) is observed on the top of the nanorod in Figure S4.a. One TD is also observed at the bottom part of the nanorod in Figure S4.b.

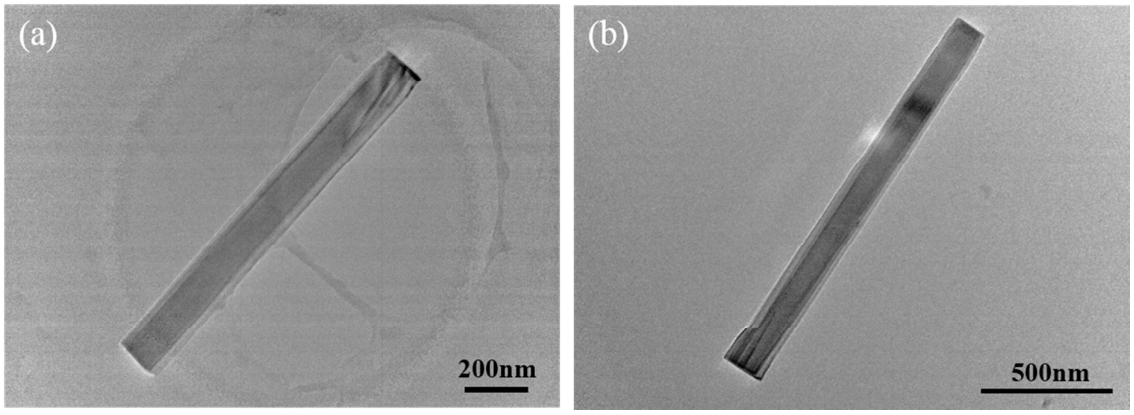

Figure S4. (a-b) TEM images of scratched AlN nanorod arrays after ICP dry etching and AZ400K wet etching.

Figure S5 displays scratched AlN faceted nanorod after MOVPE regrowth. One threading dislocation (TD) is observed at the bottom and the top of the nanorod in Figure S5.a. One pit can be observed in the nanorod in Figure S5.b, which is related to the bending of a TD toward the lateral free surface.

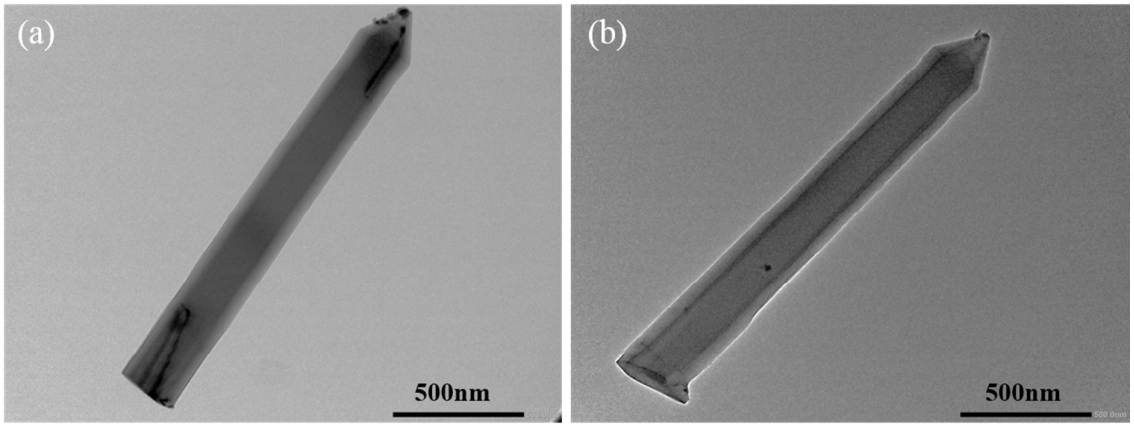

Figure S5. (a-b) TEM images of scratched AlN faceted nanorod arrays after MOVPE regrowth.

S5: *m*-plane growth rate

AlN *m*-plane growth rate has been obtained by extracting the increase of the inner radius of the regrown nanorod compared to the etched nanorod such as:

$$m - plane\ growth\ rate = (r_i^{MOVPE} - r_i^{etch})\ /\ growth\ time.$$

Note, the outer circle of a hexagon intersects each corner while the inner circle touches the middle of each facet, such that $d_i = d_o.\sqrt{3}/2$. SEM plan view pictures and TEM images of AlN nanorod before and after regrowth has been used to extract an *m*-plane growth rate of ~ 1 nm.

S6: AlN template specification provided by Nanowin

The AlN template are insulting with a thickness of 4-6 µm, a roughness inferior to 1.2 nm, and an XRD FWHM inferior to 350 and 450 arcsec, respectively for the (0002) and (10-12) reflections.

S7: Complementary CL characterization and discussion

Figure S6 displays the CL spectra acquired for the three AlGaN SQW samples for a broad range of energy. In addition to the AlN NBE and the AlGaN SQW emission already extensively discussed in the manuscript, a lower energy broad emission band is observed between 2.6 and 4.3eV for all samples (Figure S6). This contribution, initially observed in the AlN template,[2] could be related to O-complexes and/or Si-complexes and other native defects, such as vacancies.

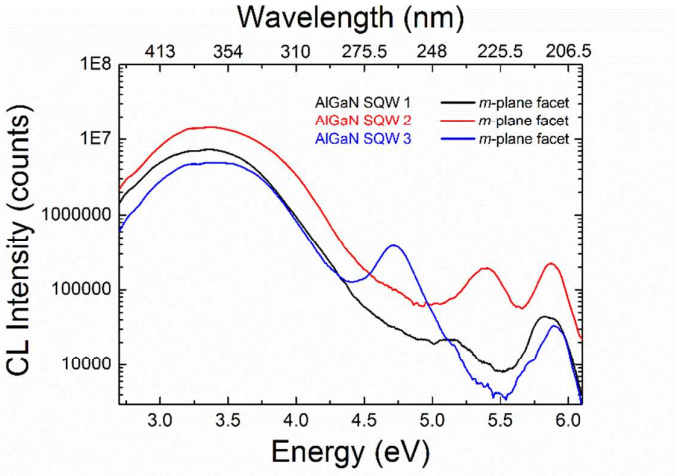

Figure S6. CL spectra acquired for the three AlGaN SQWs showing emission from the *m*-plane nanorod sidewalls.

The high intensity of the defect luminescence is partly due to the low vacuum mode in which the CL images where acquired. In low vacuum mode, water vapour is released into the chamber, which is ionised by the electron beam which in turn helps to disperse charge building up on the sample surface (Figure S7.b). This has the side effect that the electron beam will interact with the gas, creating an (low density) electron skirt around the beam spot. Beam electrons in the skirt will be able to recombine radiatively in the same way as electrons in the main beam. This leads to an overestimation of the contribution of the defect luminescence to the total intensity as defect centres are very efficient carrier traps (Figure S7.c).

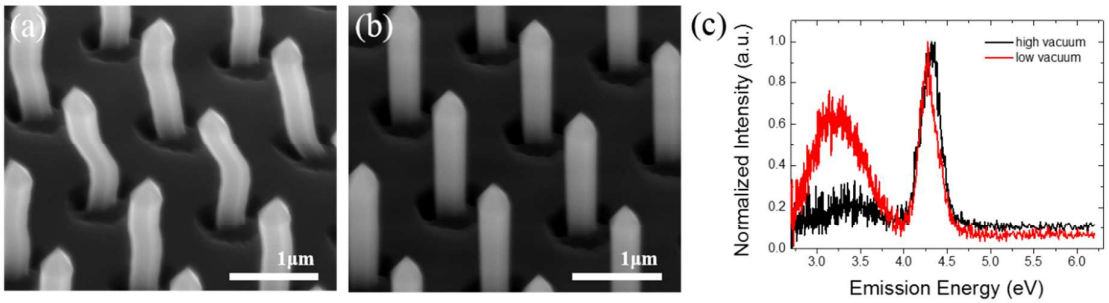

Figure S7. SEM images of nanorods with an AlGaN SQW in (a) high vacuum and (b) low vacuum. CL spectra of the same nanorod acquired in low and high vacuum mode. (Note, for a different AlGaN SQW sampel as in the main paper).

To demonstrate this effect, CL measurements at high vacuum and low vacuum have been carried out under the same conditions on the same sample area (optimized for high vacuum CL thus lower beam current, to prevent charging effects) and are presented in Figure S7.

Figure S8 shows a line spectrum extending from the top to the bottom of the nanorod for the three AlGaN SQW samples, displayed on a log scale and for a broad range of energy. As already observed in Figure S6, the high intensity of the defect band dominates the linescan, with a uniform emission across the height of the nanorod. The fluctuation of the intensity between AlGaN SQW samples observed for both the defect band and the AlN NBE emission could be related to the introduction of points defects in the regrown AlGaN/AlN shell.

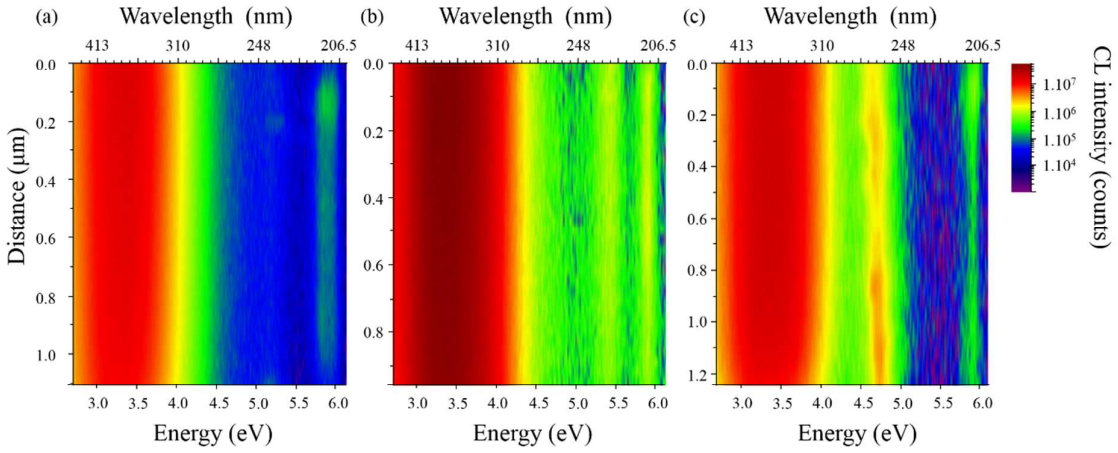

Figure S8. Log-scale RT spectral line-spectrum extracted along the length of the nanorod for (a) AlGaN SQW 1, (b) AlGaN SQW 2 and (c) AlGaN SQW 3.

[1] Solak, H. H; Dais, C; Clube, F. Displacement Talbot lithography: a new method for high-resolution patterning of large areas. *Opt. Express* **2011**, 19, 10686-10691.
[2] Coulon, P.-M.; Kusch, G.; Le Boulbar, E. D.; Chausse, P.; Bryce, C.; Martin R. W.; Shields, P. A. Hybrid Top-Down/Bottom-Up Fabrication of Regular Arrays of AlN Nanorods for Deep-UV Core-Shell LEDs. *Phys. Status Solidi B* **2017**, 6, 599–602.